Hydrostatically Extruded Glass Fiber Reinforced Polyoxymethylene. II: Modeling the Elastic Properties

P. J. HINE, S. WIRE, R. A. DUCKETT, *and* I. M. WARD

IRC in Polymer Science and Technology
University of Leeds
Leeds LS2 9JT United Kingdom

This paper describes an investigation into modeling the elastic properties of hydrostatically extruded short glass fiber reinforced polyoxymethylene (POM). The starting material for the extrusion was randomly arranged short glass fibers (25 wt%, average length 150 μm) in an isotropic POM matrix. Extrusion was carried out through a reducing conical die at 15°C below the melting point of the matrix phase (hence the composite was extruded in the solid state), such that after extrusion, preferential alignment along the extrusion direction was developed for both the fibers and for the crystalline fraction of the polymer matrix. The elastic properties of samples, made over a range of extrusion ratios, were measured using the ultrasonic immersion method, a technique that allows a complete set of elastic constants to be determined for a composite. Theoretical predictions for the elastic properties of the oriented extrudates were generated by combining a modification to the theory of Wilczynski to allow for the fibers' being surrounded by an oriented matrix phase, together with the aggregate model of Ward to model the effects of partial orientation of the fiber oriented matrix units.

INTRODUCTION

While many published research studies have explored the effects of a preferred fiber orientation distribution on composite mechanical properties, few have reported the development of matrix orientation during composite processing, and even fewer have attempted to model the effects of both fiber and matrix orientation on composite elastic properties. In a previous paper (1) we described the development of fiber and matrix orientation during the solid state hydrostatic extrusion of short glass fiber filled polyoxymethylene (POM). The material was extruded in circular cross section through a conical die of semi-angle 15°, producing rods at a range of extrusion ratios up to 6.91. Fiber orientation of the extrudates was measured using image analysis of polished sections, while matrix orientation was measured using X-ray diffraction techniques. The measured fiber and matrix orientation distributions were compared with theoretical predictions, calculated from the imposed deformations using the pseudo-affine deformation scheme (2). It was shown that the changes in fiber orientation due to extrusion were close to those predicted by the pseudo-affine deformation scheme (particularly for the highest extrusion ratios), whereas the orientation of the crystalline regions of the POM matrix were found to be significantly higher than the theoretical predictions.

In this paper we continue this study by examining the effect of the changes in fiber and matrix orientation on the elastic properties of the extrudates. Of particular interest is to model the elastic properties of the composites in light of the preferred but different levels of orientation for the fibers and for the crystalline portion of the matrix.

The experimental values of the elastic properties of the extrudates were determined using the ultrasonic immersion method. This technique has been used extensively in this and other laboratories for structure/property investigations of unidirectional and short fiber composites (e.g. 3–5) because it allows a full description of the elastic properties of an anisotropic material to be determined, and hence provides a more rigorous test of new modeling procedures. A possible drawback of the ultrasonic immersion method is its apparent insensitivity to fiber length. Experiments on a number of "short" fiber composite systems (e.g. 5, 6) have shown that excellent correlation is found between experimentally determined composite elastic constants using the ultrasonic immersion method and theoretical predictions calculated on the basis of an infinitely long fiber. This paradox is currently under investigation and no firm conclusion has yet been reached.

In this study we confine ourselves to developing a "long" fiber model to form the theoretical estimates of

the extrudate elastic properties, which are then compared with the ultrasonic experimental results. This allows for a full discussion of the effects of fiber and matrix orientation on the composite elastic properties, but ignores the effects of the fiber aspect ratio on composite elastic properties.

EXPERIMENTAL

Hydrostatic Extrusion

The starting material was CELCON, short glass fiber filled polyoxymethylene (POM) copolymer, supplied by Hoechst Celanese Research Company. The grade was GC-25; isotropic POM (MFI = 2.5) filled with 25 wt% (14 vol%) of nominally randomly arranged short glass fiber. The average starting fiber length was 150 μm, which was measured to be reduced to 133 μm after extrusion: the average fiber diameter was 12.5 μm.

Extrusion was carried out at 150°C (15°C below the melting point of the polymer) at a rate of 10 mm/min: the polymer was therefore in the solid phase during the extrusion process. In this paper we compare three extrusion ratios, 3.65, 5.31, and 6.91, with the isotropic starting material [In the previous paper (1) we reported results on a further material of a lower draw ratio = 1.77. However, as this material was subsequently discovered to be of a lower fiber volume fraction than the other materials, it could not be included in the studies of mechanical properties]. In addition to the glass-filled grades, a sample of a comparable unfilled grade of POM (M25-01) has been extruded at a ratio of 6.2 (a nominal extrusion ratio of 8). Further details of the hydrostatic extrusion of glass-filled POM can be found elsewhere (1, 7).

Fiber and Matrix Orientation

The previous paper (1) concentrated on developing a procedure for the accurate measurement of fiber orientation in these extrudates. The chosen technique was image analysis of polished sections taken from the composite, using a transputer controlled image analyzer built for this purpose by the Instrumentation Group at Leeds University (8, 9). From the analysis of each elliptical fiber footprint on a given section, the two angles that specify the three-dimensional orientation of each fiber, θ and ϕ, are determined. If we define a set of orthogonal axes such that the 3 axis is parallel to the extrusion direction, while the 1 and 2 axes are perpendicular to this, then angle θ is defined as the angle a fiber makes with the extrusion direction, and angle ϕ is defined as the angle a fiber makes when projected onto the 12 plane. All the extrudates were found to be predominantly transversely isotropic, as would be expected for extruded circular rods, so that there was no preferred ϕ orientation (i.e. no preferred orientation in the 12 plane). Fiber orientation and matrix orientation could therefore be totally defined in terms of angle θ. It was shown in the previous paper that to obtain the most accurate fiber orientation measurements for the oriented extrudates, a section at an angle to the extrusion section is required. The most appropriate section angle was chosen by first analyzing a transverse section (i.e., in the 12 plane) from each extruded rod.

The orientation of the crystalline fraction of the matrix was measured using a Huber X-ray diffractometer, from analysis of the {008} meridional reflection. From the fiber measurements it was safe to assume that the matrix orientation would be transversely isotropic, and therefore only the orientation with respect to the extrusion direction (specified by the angle θ) was measured.

Because of the transverse isotropy of these rod extrudates, only two orientation averages were needed to specify the orientation of the fibers and the crystalline portion of the matrix: $\langle\cos^2\theta\rangle$ and $\langle\cos^4\theta\rangle$. A summary of the measured orientation values, for both the fibers and the matrix crystals, is shown in *Table 1*.

Measurement of Elastic Properties

The elastic properties of the extrudates were measured using the ultrasonic velocity method, developed by Lord (10), based on the initial work by NPL (11). As described in the **Introduction**, this technique has been used extensively in this laboratory for the development of modeling schemes, and enables a full description of the elastic anisotropy of a composite. The sample to be tested is placed between an ultrasonic transmitter and receiver (2.25 MHz) in a water bath set at 25°C, and the time for an ultrasonic pulse to travel between the two transducers is measured. The unique aspect of the technique is that for non-normal incidence, mode conversion at the liquid/solid interface can cause the incident longitudinal wave (usually termed the L wave) to be split into a longitudinal and a transverse or shear wave (T wave) inside the sample. Measurement of the transit time for a range of incidence angles allows the velocities of these two waves to be measured. Two equations relate the velocity/angle relationship of these two waves to the four stiffness constants in the plane of wave propagation.

For example, for propagation in the 23 plane

$$V_L^2 = \frac{B_{11} + B_{22} + [(B_{11} - B_{22}) + 4B_{12}^2]^{\frac{1}{2}}}{2\rho} \quad (1)$$

$$V_T^2 = \frac{B_{11} + B_{22} - [(B_{11} - B_{22}) + 4B_{12}^2]^{\frac{1}{2}}}{2\rho} \quad (2)$$

Table 1. Measured Orientation Averages for the Fibers and the Crystalline Portion of the Matrix.

Extrusion Ratio	Fiber Orientation Filled Extrudates		Matrix Orientation Filled Extrudates	
	$\langle\cos^2\theta\rangle$	$\langle\cos^4\theta\rangle$	$\langle\cos^2\theta\rangle$	$\langle\cos^4\theta\rangle$
1.77	0.666	0.530		
3.65	0.857	0.773	0.900	0.830
5.31	0.896	0.833		
6.91	0.926	0.878	0.953	0.919

where

$$B_{11} = (C_{33}\cos^2 r + C_{44}\sin^2 r)$$

$$B_{22} = (C_{22}\cos^2 r + C_{44}\sin^2 r)$$

$$B_{12} = (C_{44} + C_{23}).\sin r.\cos r$$

C_{ij} here are the unknown stiffness constants of the sample, ρ is the material density, and r is the angle of refraction. Therefore, if a rectangular sample (3 mm thick) is cut from the center of an extruded rod, placed between the sound transducers with its 3 axis horizontal, velocity/angle measurements taken by rotating the sample around its 1 axis will result in the determination of the stiffness constants C_{33}, C_{22}, C_{44} and C_{23} from a fitting procedure using *Equations 1* and *2*. Rotating the sample through 90° so that the 3 axis (the extrusion direction) is vertical and repeating the measurements gives values for the stiffness constants C_{11}, C_{22}, C_{66}, and C_{12} (sound propagation in the 12 plane). These two experiments give the five elastic constants needed for a full description of the elastic properties of a transversely isotropic material: C_{11}, C_{33}, C_{13}, C_{12}, and C_{44}.

THEORY

The modeling procedure for predicting the properties of partially aligned fiber reinforced composites is usually undertaken in two stages. The first is the determination of the properties of the composite structural unit, and the second is to calculate the effects of the misorientation of these units. Many theories exist for the determination of the properties of the composite structural unit, in varying degrees of sophistication. In a previous paper, on well-aligned short carbon fiber reinforced composites (12), we showed that although the most thorough route to predicting the elastic properties of the structural unit was by a finite element technique based on the work of Zhang and Evans (13), this was a time consuming process. The paper concluded that the analytical theory of Wilczynski (13, 14) gave the optimum predictions in terms of ease of use and speed of calculation. The Wilczynski approach has the advantage that it can be easily modified to allow anisotropic fiber and matrix phases to be implemented for the composite unit, as required here, something that is not easily accomplished for most of the other currently available structural unit theories.

In the Wilczynski model the composite structural unit is envisaged as a cylindrical fiber encased in a cylindrical sheath of matrix. Simple loading cases of this unit are chosen that have well-known elasticity solutions in cylindrical coordinates, as described by Timoshenko and Goodier (15), allowing the elastic properties of the unit to be determined. Here, a simple modification has been made to the most recent paper of Wilczynski (14), which allowed for a transversely isotropic fiber and an isotropic matrix, to describe the general case of a transversely isotropic fiber and transversely isotropic matrix; of course in this paper the fiber was isotropic. While it is outside the scope of the current discussion to develop the relevant equations fully, the necessary modifications to the main equations of the theory are included in the **Appendix**. It is a relatively simple matter to program these equations into a spreadsheet to obtain the five elastic constants required for a full description of the elastic properties of the unit.

The properties of the composite can now be determined by averaging the unit properties in terms of the measured orientation distributions. This is achieved using the aggregate model proposed by Ward (16) and developed for composites by Brody and Ward (17). It assumes that the composite consists of an aggregate of units whose orientation is specified by orientation averages of the angles θ and ϕ (defined earlier). This formulation is equivalent to the later treatment by Advani and Tucker (18). Orientation averaging can be done either in terms of the stiffness constants C_{ij} or the compliance constants S_{ij} (equivalent to assuming constant strain or constant stress within the aggregate), leading to upper and lower bound predictions. Where the orientation in the composite shows transverse isotropy, as here, the orientation of the units depends only on the angle θ and the aggregate model can be simply expressed. For example, for averaging the compliance constants, the relevant equations are as follows:

$$S'_{33} = S_{11}\langle\sin^4\theta\rangle + S_{33}\langle\cos^4\theta\rangle + (2S_{13} + S_{44}) \cdot \langle\sin^2\theta.\cos^2\theta\rangle \quad (3)$$

$$S'_{11} = \frac{1}{8}(3\langle\cos^4\theta\rangle + 2\langle\cos^2\theta\rangle + 3)S_{11} + \frac{1}{4}(3\langle\sin^2\theta\cos^2\theta\rangle + \langle\sin^2\theta\rangle)S_{13} + \frac{3}{8}\langle\sin^4\theta\rangle S_{33} + \frac{1}{8}(3\langle\sin^2\theta\cos^2\theta\rangle + \langle\sin^2\theta\rangle)S_{44} \quad (4)$$

$$S'_{13} = \frac{1}{2}\langle\sin^2\theta\cos^2\theta\rangle S_{11} + \frac{1}{2}\langle\sin^2\theta\rangle S_{12} + \frac{1}{2}(\langle\sin^4\theta\rangle + \langle\cos^4\theta\rangle + \langle\cos^2\theta\rangle)S_{13} + \frac{1}{2}\langle\sin^2\theta\cos^2\theta\rangle S_{33} - \frac{1}{2}\langle\sin^2\theta\cos^2\theta\rangle S_{44} \quad (5)$$

$$S'_{12} = \frac{1}{8}(\langle\cos^4\theta\rangle - 2\langle\cos^2\theta\rangle + 1)S_{11} + \langle\cos^2\theta\rangle S_{12} + \frac{1}{4}(\langle\sin^2\theta\cos^2\theta\rangle + 3\langle\sin^2\theta\rangle)S_{13} + \frac{1}{8}\langle\sin^4\theta\rangle S_{33} + \frac{1}{8}(\langle\sin^2\theta\cos^2\theta\rangle - \langle\sin^2\theta\rangle S_{44} \quad (6)$$

$$S'_{44} = (2\langle\sin^2\theta\cos^2\theta\rangle + \langle\sin^2\theta\rangle)S_{11} - \langle\sin^2\theta\rangle S_{12} - 4\langle\sin^2\theta\cos^2\theta\rangle S_{13} + 2\langle\sin^2\theta\cos^2\theta\rangle S_{33} + \frac{1}{2}(\langle\sin^4\theta\rangle + \langle\cos^4\theta\rangle - 2\langle\sin^2\theta\cos^2\theta\rangle + \langle\cos^2\theta\rangle)S_{44} \quad (7)$$

where S_{ij} are the compliance constants of the unit, S'_{ij} are the calculated compliance constants of the aggregate (or the composite) and $\langle\cos^2\theta\rangle$ etc. are the measured orientation averages. A similar set of five equations can be derived for averaging the stiffness constants C_{ij}.

For the extruded glass/POM composites examined in this study there are a number of challenges to the use of the aggregate model for orientation averaging caused by the presence of the oriented matrix phase. First, as shown in *Table 1*, the measured level of orientation is different for the two phases, with the crystalline portion of the matrix more highly aligned than the fibers at a particular extrusion ratio. It is therefore not correct, in principle, to chose a single level of misorientation for each unit, be it from the measured fiber orientation or from the measured matrix orientation. However, it will be shown below that the differences in the theoretical predictions caused by using the two different levels of orientation at a particular extrusion ratio are small and that the most effective solution is to use the measured fiber orientation for the theoretical predictions.

A second problem relates to the morphological changes in the POM matrix caused by the solid phase extrusion process. Such changes during the solid phase deformation of unfilled crystalline polymers, reported by a number of previous authors (20, 21), are usually attributed to the breaking up of the original crystalline lamellae and the gradual transformation into a fibrillar structure, and so cannot be modeled purely in terms of changes in orientation. As a consequence it is not possible to predict the properties of the isotropic polymer by using the aggregate model and the properties of the most highly oriented material. This is also true for the filled material, with the result that the assumption of random orientation of a unit composed of the most highly aligned POM matrix around a glass fiber does not predict the properties of the isotropic starting composite material.

The third problem, which has the effect of mitigating the first two problems, is that the matrix orientation measured by X-ray diffraction relates only to the crystalline portion of the matrix. As the POM matrix is ≈70% crystalline, there is a remaining 30% of amorphous material, which will be much less oriented.

RESULTS AND DISCUSSION

Isotropic Matrix

As a check on the modeling procedures, the first material to be examined was the starting material for the extrusion process: random glass fibers in an isotropic POM matrix. Ultrasonic measurement of the elastic properties was carried out, both for the starting composite and for the unfilled matrix material: the latter is needed for determination of the unit properties. *Table 2* shows the results of the ultrasonic tests for the unfilled and filled isotropic POM matrix. Both the engineering constants (Young's modulus E, Poisson's ratio ν, and shear modulus G) and the stiffness constants C_{33}, C_{13}, and C_{44} are shown (only two of these are independent for an isotropic material as $G = E/2.(1 + \nu)$ and $C_{44} = (C_{33} - C_{13})/2$). For this, and all subsequent comparisons between experiment and theory, the stiffness constants are used because these are directly measured using the ultrasonic technique.

Figure 1 shows a comparison between the experimentally measured stiffness constants and the theoretical predictions. In this, and all the following *Figures*, the experimental values are shown as filled circles and the theoretical bounds are shown in the form of error bars. The theoretical values were determined using the Wilczynski model for the unit properties and the aggregate model, with a random arrangement of fibers, to form the composite predictions. (As discussed in the **Introduction**, in the ultrasonic immersion test the fibers appear infinitely long, so in all the following modeling comparisons no account has been made of the fiber aspect ratio.) The glass fiber properties used in all the calculations were a Young's modulus of 72.5 GPa and a Poisson's ratio of 0.2: the glass fiber volume fraction was 0.136. *Figure 1* shows that the agreement between theory and experiment, for the starting material, was excellent, validating the modeling procedures.

Aligned Matrix

Table 3 shows the elastic properties of the extruded composites, together with the properties of unfilled polyoxymethylene extruded at the highest draw ratio achievable (nominal extrusion ratio = 8.0 – actual extrusion ratio due to die swell = 6.20). The X-ray diffraction measurements of the matrix crystalline orientation in the unfilled extrudate are found to be almost identical to those for the filled extruded material (filled $\langle\cos^2\theta\rangle$ = 0.953: unfilled $\langle\cos^2\theta\rangle$ = 0.962). The elastic properties of the unfilled extrudate can therefore be taken as a good representation of the properties of the matrix in the filled extrudate.

Table 2. The Measured Elastic Properties of the Unfilled and Random Glass Filled Polyoxymethylene.

	Unfilled POM	Random Fibers/Isotropic POM		Unfilled POM	Random Fibers/Isotropic POM
E	3.97	6.49	C_{33}	7.57	10.3
ν	0.383	0.348	C_{13}	4.69	5.52
G	1.44	2.41	C_{44}	1.44	2.41

Glass Fiber E = 72.5 GPa, ν = 0.2.
Fiber volume fraction = 0.136.

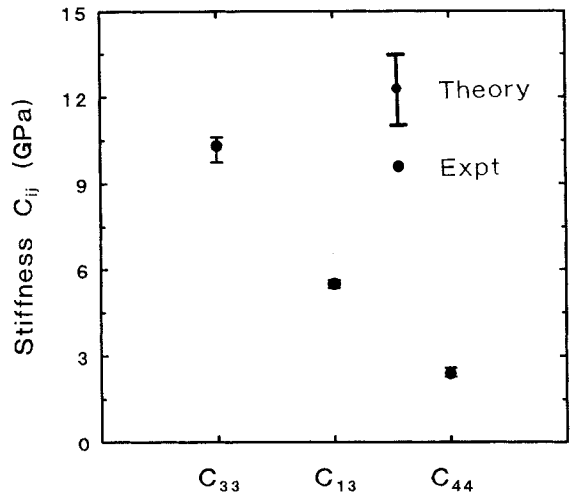

Fig. 1. A comparison between theory and experiment for the starting material: random glass fibers in an isotropic matrix.

Table 3. The Measured Stiffness Constants of the Filled and Unfilled Extrudates.

	Unfilled POM M25-01 ER = 6.20	Filled POM GC-25 ER = 3.65	Filled POM GC-25 ER = 5.31	Filled POM GC-25 ER = 6.91
C_{33}	10.9	15.8	18.1	18.9
C_{11}	8.15	8.79	9.52	9.52
C_{13}	5.29	5.00	5.50	5.54
C_{12}	4.88	5.09	5.15	5.23
C_{44}	1.83	2.31	2.30	2.48

The theoretical estimates of the composite elastic properties can now be undertaken by combining the modified Wilczynski model with the aggregate model. To form the unit we need to surround the fiber with the appropriate matrix properties. In light of the high degree of matrix orientation measured for the extruded unfilled POM, it would be perfectly valid to use these elastic properties. However, for completeness, we have elected to determine the properties of the most highly aligned matrix ($\langle\cos^2\theta\rangle = 1$) by using the aggregate model in reverse. *Equations 3* to *7* express the properties of the aggregate S'_{ij} (normally unknown) in terms of the properties of the aligned unit S_{ij} and the orientation averages (both normally known). For the extruded matrix the properties of the misaligned aggregate are known, as are the orientation averages, which allows *Equations 3–7* to be expressed as simultaneous equations and solved for the highly aligned properties S_{ij}. *Table 4* shows the results of this calculation and indicates that in terms of the measured elastic constants, only E_{33} is significantly lower than would be expected for the fully aligned matrix: the other four elastic constants are little affected by the small decrease in orientation. The properties of the unit have been determined from the modified Wilczynski equations as shown in the **Appendix**, using the "fully aligned" elastic constants in *Table 4*.

In forming the aggregate predictions there are two remaining questions. The first is that the fibers and

Table 4. Calculation of the Elastic Properties of the Most Highly Aligned Matrix.

	Misaligned Properties (Measured)	Fully Aligned Properties		
		Lower Bound	Upper Bound	Average
E_{33}	6.62	6.68	7.12	6.90 ± 0.22
E_{11}	4.62	4.55	4.65	4.60 ± 0.05
ν_{13}	0.406	0.405	0.415	0.410 ± 0.05
ν_{12}	0.415	0.423	0.427	0.425 ± 0.002
G_{13}	1.83	1.78	1.82	1.80 ± 0.02

the crystalline regions of the matrix have been shown (*Table 1*) to have different levels of orientation for use in *Equations 3–7*. Simulations using the two different measures of orientation (i.e. fiber and matrix) have shown that the differences in the final predictions are small (<1%). There is the additional fact that the orientation measured for the matrix relates only to the crystalline portion, and that the overall orientation is likely to be slightly lower. In light of these two results we have elected to determine the aggregate predictions using the fiber orientation averages.

First let us consider the extrudate with the highest extrusion ratio (6.91). Comparison between experiment and theory for this material allows the validity of the unit predictions to be checked, because at the high level of orientation seen in this material, using the aggregate model does not influence matters significantly. *Figure 2* shows that there is excellent agreement between all five experimentally measured stiffness constants and the theoretical predictions, thus validating the extension to the Wilczynski model to include an aligned matrix.

Figure 3a shows a comparison between the experimentally measured values of C_{33} and the theoretical predictions (upper and lower bounds shown) for all the materials. The measured values are seen to fall inside the predicted bounds, with the highest draw ratio (6.91) close to the upper bound and the lowest

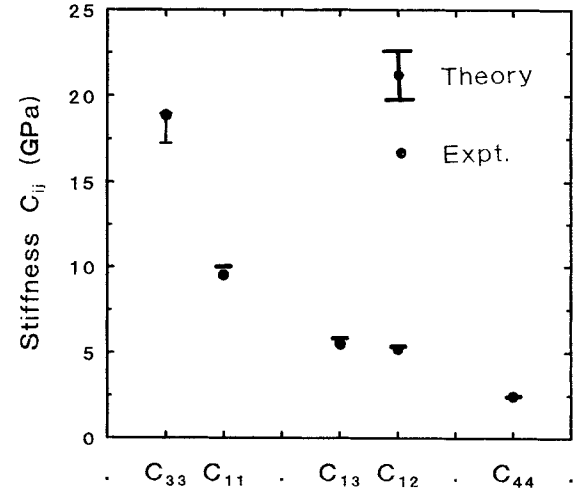

Fig. 2. A comparison between theory and experiment for the highest extrusion ratio.

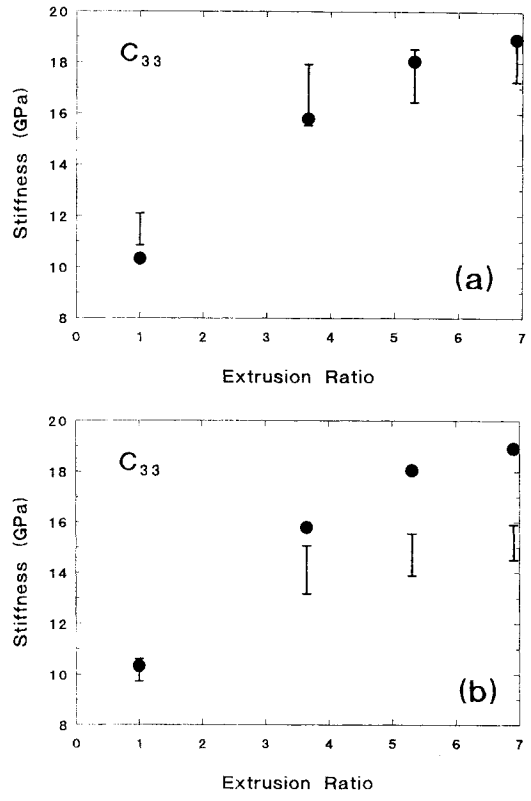

Fig. 3. A comparison between theory and experiment for the axial stiffness C_{33}, using a composite structural unit with a) highly aligned matrix to surround the fiber and b) isotropic matrix to surround the fiber.

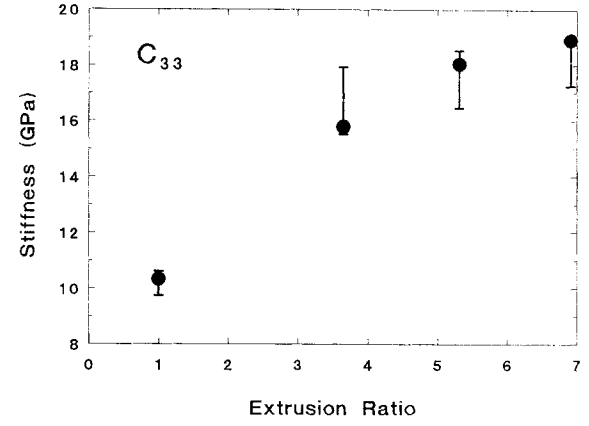

Fig. 4. A comparison between theory and experiment for the axial stiffness C_{33}, using isotropic matrix around the fiber for the starting material and highly aligned matrix around the fiber for the extrudates.

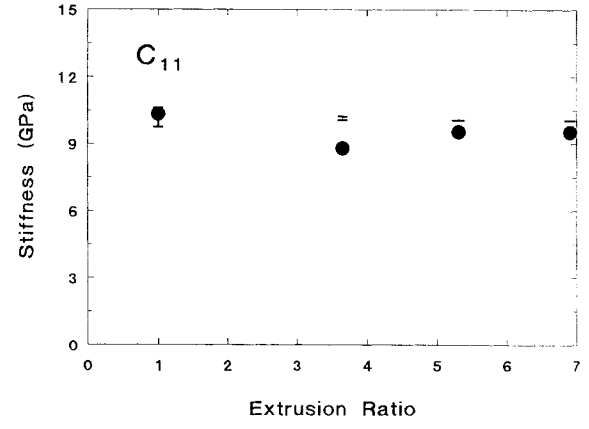

Fig. 5. A comparison between experiment and theory for C_{11}.

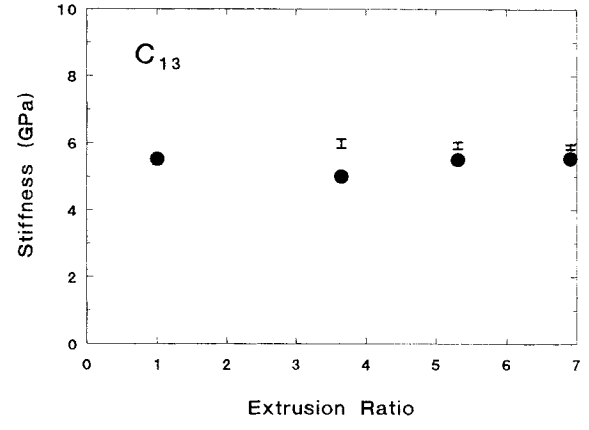

Fig. 6. A comparison between experiment and theory for C_{13}.

draw ratio (3.65) close to the lower bound. As mentioned in the **Theory** section, randomizing the aligned matrix unit does not predict the properties of the starting material (extrusion ratio = 1), as a result of changes in the structure of the matrix due to the extrusion process. If the fiber is surrounded by isotropic matrix and then averaged according to the measured fiber orientation distributions, then the theory predicts the properties of starting material very well, as shown earlier in *Fig. 1*, but underestimates the value of C_{33} for the extruded materials (*Fig. 3b*). The best agreement is therefore obtained by surrounding the fiber with the most highly aligned matrix properties for predicting the oriented extrudate properties and with the isotropic matrix for predicting the isotropic starting material. *Figure 4* shows the results presented in this way.

Figures 5 to *8* show comparisons between the measured elastic properties, and theoretical predictions, for C_{11}, C_{13}, C_{12}, and C_{44}, respectively. As for *Fig. 4*, the starting material is predicted using an isotropic matrix to surround the fiber, and the extrudates are modeled using the highly aligned matrix. The most general conclusion from these four graphs is that the changes in fiber and matrix orientation produced by the extrusion process have little effect on these four elastic constants. While the agreement between experiment and theory is generally good, it is best either when either the matrix is isotropic (ER = 1) or the fibers and matrix are highly aligned (ER = 6.91). Misorienting the aligned matrix unit to the desired value for the intermediate extrusion ratios produces a small overestimate of the stiffness constants, which is worse the lower the degree of orientation. This discrepancy between the theoretical predictions and the ultrasonic measured constants, particularly C_{12}, is somewhat

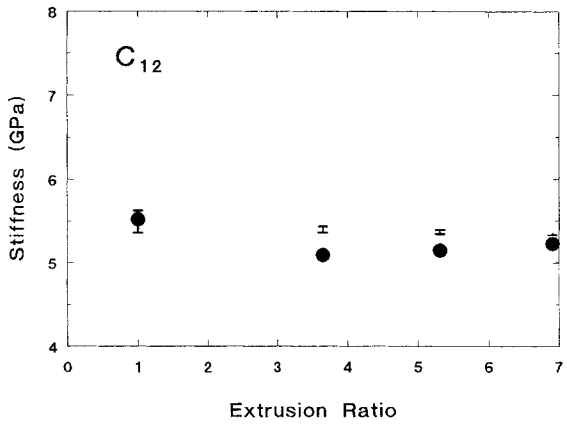

Fig. 7. A comparison between experiment and theory for C_{12}.

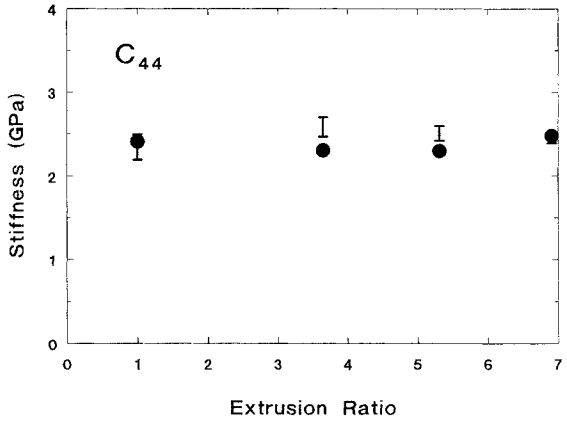

Fig. 8. A comparison between experiment and theory for C_{44}.

reminiscent of the data presented by Chan *et al.* (21) in their measurement (again using ultrasonics) of the stiffness constants of extruded unfilled poly(ethylene terephthalate). The authors attributed the differences to the morphological changes that occur in the matrix during solid state extrusion, and these results tend to confirm those suppositions.

CONCLUSIONS

The Wilczynski model for predicting the elastic properties of the composite structural unit has been extended to allow for the general case of transversely isotropic fibers and a transversely isotropic matrix. Together with the aggregate model of Ward, this has been shown to give excellent theoretical predictions for the changes in the axial stiffness of glass fiber reinforced polyoxymethylene composites produced by solid state extrusion at a range of extrusion ratios. The properties of the most highly aligned matrix material, needed to surround the fiber when determining the unit properties, has been calculated by using the aggregate model of Ward in reverse. As has been noted before by ourselves and other authors, the other four stiffness constants of these transversely isotropic rod extrudates are little affected by significant changes in either fiber or matrix orientation.

APPENDIX

This appendix presents the necessary modifications to the theory of Wilczynski (14) to allow for the general case of a transversely isotropic fiber and matrix.

The axis system used here is as defined by Wilczynski and not as used throughout the rest of this paper. This should allow direct comparison with the full development of the theory described by Wilczynski (14). Therefore the 1 axis is defined as the fiber axis, with the 3 and 2 axes in the isotropic plane of the unit.

In the Wilczynski theory, four selected loading cases are chosen that lead to the determination of the five independent elastic constants of the unit. These are:

Case 1: simple tension in the direction of the fiber axis.

Case 2: plane homogeneous compression in the isotropic plane of the unit.

Case 3: pure shear in the isotropic plane of the unit.

Case 4: pure shear parallel to the fiber axis.

The modification to the equations in Wilczynski (14) to allow for the most general case of transverse isotropic fiber and matrix are therefore as follows:

CASE 1:

Replace *Eq 7* in Wilczynski (14)

$$F + G = 0$$

$$[(1 - \nu_{23}^f) + (1 + \nu_{23}^m)k]F + [(1 - \nu_{23}^f) - (1 - \nu_{23}^m)k]fG + [(1 - f).\nu_{12}^f + \nu_{12}^m fk]\sigma_{xx} = \nu_{12}^f$$

$$2\nu_{21}^f F + 2(\nu_{21}^f - \nu_{21}^m l)fG + ((1 - f) + lf)\sigma_{xx} = 1$$

where

f = fiber volume fraction

$$k = \frac{E_{22}^f}{E_{22}^m}$$

$$l = \frac{E_{11}^f}{E_{11}^m}$$

CASE 2:

Replace *Eq 8* in Wilczynski (14)

$$F + G = -1$$

$$[(1 - \nu_{23}^f) + (1 + \nu_{23}^m)k]F + [(1 - \nu_{23}^f) - (1 - \nu_{23}^m)k]fG + [(1 - f)\nu_{12}^f + \nu_{12}^m fk]\sigma_{xx} = 0$$

$$2\nu_{21}^f F + 2(\nu_{21}^f - \nu_{21}^m l)fG + ((1 - f) + lf).\sigma_{xx} = 0$$

CASE 3:

Replace *Eq 14* in Wilczynski (14)

$$A + 3.B + D = -1$$

$$B - C - D = 0$$

$$[(1 + \nu_{23}^f) - (1 + \nu_{23}^m)k]f^2A + [4(\nu_{23}^f + \nu_{12}^f\nu_{21}^f) - 4k(\nu_{23}^m + \nu_{12}^m\nu_{21}^m)]f^3B + [3(1 + \nu_{23}^f) - 4(\nu_{23}^f + \nu_{12}^f\nu_{21}^f) + k(1 + \nu_{23}^m)]C + [4(1 + \nu_{23}^f) - 4(\nu_{23}^f + \nu_{12}^f\nu_{21}^f) + 4k(1 - \nu_{12}^m\nu_{21}^m)]fD = 0$$

$$[(1 + \nu_{23}^f) - (1 + \nu_{23}^m)k]f^2A + [2(3 - 2\nu_{12}^f\nu_{21}^f + \nu_{23}^f) - 2k(3 - 2\nu_{12}^m\nu_{21}^m + \nu_{23}^m)]f^3B + [3(1 + \nu_{23}^f) - 2(3 - 2\nu_{12}^f\nu_{21}^f + \nu_{23}^f) - k(1 + \nu_{23}^m)]C + [4(1 + \nu_{23}^f) - 2(3 - 2\nu_{12}^f\nu_{21}^f + \nu_{23}^f) + 2k(1 - \nu_{23}^m - 2\nu_{12}^m\nu_{21}^m)]fD = 0$$

CASE 4:

Replace *Eq 20* in Wilczynski (14)

$$G_{12}^c = G_{12}^m \frac{G_{12}^f(1 + f) + G_{12}^m(1 - f)}{G_{12}^f(1 - f) + G_{12}^m(1 + f)}$$

REFERENCES

1. P. J. Hine, N. Davidson, R. A. Duckett, A. R. Clarke, and I. M. Ward, *Polym. Compos.*, **17,** 720 (1996).
2. I. M. Ward, *Mechanical Properties of Solid Polymers*, 2nd Ed., p. 286, J. Wiley and Sons, Chichester, England (1983).
3. S. R. A. Dyer, D. Lord, I. J. Hutchinson, I. M. Ward, and R. A. Duckett, *J. Phys. D: Appl. Phys.*, **25,** 66 (1992).
4. P. W. A. Stijnman, *Composites*, **26,** 597 (1995).
5. P. J. Hine, R. A. Duckett, I. M. Ward, P. S. Allan, and M. J. Bevis, *Polym. Compos.*, **17,** 400 (1996).
6. S. Wire, Internal report for General Motors, 1996.
7. P. S. Hope, A. Richardson, and I. M. Ward, *Polym. Eng. Sci.*, **22,** 307 (1982).
8. A. R. Clarke, N. Davidson, and G. Archenhold, *Proceedings of Transputing '91*, 1 (1991).
9. A. R. Clarke, N. Davidson, and G. Archenhold, *Trans. Royal Microscopial Soc.*, **1,** 305 (1990).
10. D. Lord, PhD Thesis, University of Leeds (1989).
11. B. E. Read and G. D. Dean, *The Determination of the Dynamic Properties of Polymers and Composites*, Adam Hilger Ltd., Bristol, England (1978).
12. P. J. Hine, R. A. Duckett, and I. M. Ward, *Compos. Sci. Technol.*, **49,** 13 (1993).
13. A. P. Wilczynski, *Compos. Sci. Technol.*, **38,** 327 (1990).
14. A. P. Wilczynski and J. Lewinski, *Compos. Sci. Technol.*, **55,** 139 (1995).
15. S. Timonshenko and N. Goodier, *Theory of Elasticity*, McGraw-Hill, New York (1951).
16. I. M. Ward, *Proc. Phys. Soc.*, **80,** 1176 (1962).
17. H. Brody and I. M. Ward, *Polym. Eng. Sci.*, **11,** 139 (1971).
18. S. G. Advani and C. L. Tucker, *J. Rheol.*, **31,** 751 (1987).
19. P. R. Pinnock and I. M. Ward, *Br. J. Appl. Phys.*, **7,** 575 (1966).
20. A. Peterlin and J. F. Balta-Calleja, *J. Appl. Phys.*, **40,** 4238 (1969).
21. O. K. Chan, F. C. Chen, C. L. Choy, and I. M. Ward, *J. Phys. D: Appl. Phys.*, **11,** 617 (1978).